A MAP EQUALIZER FOR THE OPTICAL COMMUNICATIONS CHANNEL

Wenze Xi, Tülay Adalı, and John Zweck

Department of Computer Science and Electrical Engineering
University of Maryland Baltimore County, Baltimore, MD 21250

ABSTRACT

A maximum a posteriori equalizer is presented for optical communication systems. Assuming that the span of the inter-symbol interference (ISI) does not extend beyond the neighboring bits – as is typically the case for the distortion introduced by polarization mode dispersion (PMD) – we derive the conditional probability distribution function in the electrical domain in the presence of PMD and amplifier spontaneous emission dominated noise. Simulation results with an accurate receiver model and all-order PMD show the success of the MAP equalizer in reducing the ISI due to PMD, and that the analytical conditional pdf we derive provides a good match to the actual distribution.

1. INTRODUCTION

In optical fiber communications systems, physical impairments in optical fibers, in particular, chromatic dispersion, fiber nonlinearity, polarization mode dispersion (PMD), and amplified spontaneous emission (ASE) noise from optical amplifiers, all interact, limiting the data rate and/or the transmission distances. Electronic domain processing, *i.e.*, processing of the signal after it is converted into an electrical current in the receiver, has become increasingly important in optical communications systems. Electrical domain approaches offer great flexibility in design and can be integrated into the chip sets at the receiver, reducing bulkiness. Also, they can potentially operate after the optical signal has been partially demultiplexed in time, which enables electrical processing to be done at a lower data rate, and hence at a substantially lower cost.

Equalizers based on a minimum mean-square error criterion have been shown to be effective in reducing the penalty due to PMD, which is the primary source of inter-symbol interference in installed terrestrial fiber systems [2]. The properties of these equalizers, when implemented for optical communications, are discussed in [1]. To optimize the performance of electronic equalizers, the properties of the signal and the noise in these systems must both be taken into account. Furthermore, the adaptive computation of filter coefficients at Gb/s data rates is still prohibitive with today's processing capabilities. More recently, equalizers based on maximum likelihood sequence estimation (MLSE) and maximum a posteriori (MAP) detection have been proposed for mitigating the effects of PMD [3],[4]. However, these solutions are computationally complex and rely on look-up tables generated through histograms, a very challenging task at the very low bit error rates optical systems operate at, typically on the order of 10^{-8}.

In this paper, we present an effective and practical MAP equalizer for mitigating the effects of PMD distortion in the presence of ASE noise. Given a transmitted bit pattern, We accurately calculate the conditional probability density function (pdf) of the received electrical current in the center bit, and show how it can be used to calculate the probabilities required for a MAP equalizer. Assuming that the effect that PMD has on the pulse in a bit-slot does not extend beyond its immediate neighboring bits, we use a three-bit MAP equalizer for mitigating inter-symbol interference due to PMD.

Although the Gaussian and Chi-square approximations typically made for the pdf of the electrical current in the receiver due to noise provide solutions that are analytically tractable, for realistic systems they are not accurate, especially in the tails of the distribution [5]. Using simulations based on an accurate receiver model, we show, for a fiber with PMD, that the conditional pdfs of the received electrical current provide an accurate representation of the actual distribution, which is a generalized Chi-square distribution [5]. In additon, we present simulation results that demonstrate the effectiveness of the proposed MAP equalizer, which, with its low memory requirement, provides a feasible solution for ISI mitigation in optical communications systems.

2. POLARIZATION MODE DISPERSION

Polarization mode dispersion (PMD) is the primary barrier to achieving single-channel data rates at 40 Gbit/s and above in installed terrestrial fiber systems. Random perturbations that cause loss of circular symmetry in the core and cladding of the fiber lead to birefringence and hence to PMD. The PMD-induced distortion can be considered to be a stationary random process in a system whose bit rate is on the order of Gbit/s, and, at a given frequency, can be characterized by two principal states of polarization (PSP) which propagate through the fiber with different group velocities. The delay between the propagation times of the two PSP is called the differential group delay (DGD), τ. This difference in arrival times leads to pulse broadening, *i.e.*, to ISI.

The effect of first-order PMD can be represented by the channel response $h(t) = \gamma\delta(t) + (1-\gamma)\delta(t-\tau)$, where

γ, a random variable uniformly distributed in $[0,1]$, represents the distribution of power between the PSP pair, and the DGD value, τ, is Maxwellian distributed.

Although the first-order PMD model provides a simple approximation, the accurate characterization of PMD in real fiber requires that we take higher-order PMD into account as well. For light with a fixed input state of polarization propagating through a birefringent fiber, the output state of polarization undergoes a rate of rotation on the Poincaré sphere with respect to the frequency that can be characterized by $\mathrm{d}\mathbf{s}/\mathrm{d}\omega = \mathbf{\Omega} \times \mathbf{s}$, where $\mathbf{s}$ is the unit Stokes vector describing the output polarization state and $\mathbf{\Omega}$ is the polarization dispersion vector of the fiber [7]. The magnitude of the polarization dispersion vector is equal to the DGD between the two PSP, $\tau = |\mathbf{\Omega}|$, while its direction determines the direction of the two orthogonal PSP, $\pm\mathbf{\Omega}/|\mathbf{\Omega}|$. The higher-order PMD distortion is due to the frequency dependence of the polarization dispersion vector $\mathbf{\Omega}$. To model all-order PMD, both orthogonal states of polarization need to be considered in the optical domain as we show in the development presented in the next section.

3. CHARACTERIZATION OF THE PDF

In this section, we derive an expression for the pdf of the received electrical current at an arbitrary time t. Let x and y denote the two orthogonal states of polarization in the optical domain, and $S_x(t)$, $S_y(t)$, $N_x(t)$, and $N_y(t)$ the noise free signal, and the ASE noise in these two states of polarization. Both the noise free signal and noise can be expanded in Fourier series as $S_x(t) = \sum_{k=-N/2}^{N/2-1} s_x(k) \exp(i\omega_k t)$, where $s_x(k)$ denotes the Fourier coefficients of $S_x(t)$, $\omega_k \equiv 2\pi k T_0/T$ with $T_0 = T/N$, and T is the period. Similarly, the Fourier coefficients of $S_y(t)$, $N_x(t)$, and $N_y(t)$, will be denoted by $s_y(k)$, $n_x(k)$, and $n_y(k)$, respectively. The number of Fourier coefficients in each expansion is denoted by N, which is chosen so that most of the signal energy in the bandwidth of interest is included.

A photodetector in the receiver converts the optical signal into an electrical current and can be approximated by an ideal square-law detector. The noise outside the signal bandwidth is filtered using an optical filter prior to the photodetector and an electrical filter after the photodetector. We denote the Fourier coefficients of the optical and the electrical filters by $h_{\mathrm{opt}}(k)$ and $h_{\mathrm{ele}}(k)$, respectively, and we express the output electrical current as

$$\begin{aligned} y(t) &= \kappa\{ \sum_{k,l=-N/2}^{N/2-1} h^*_{\mathrm{opt}}(k) \left[s_x(k) + n_x(k)\right]^* h_{\mathrm{opt}}(l) \cdot \\ &\quad \left[s_x(l) + n_x(l)\right] h_{\mathrm{ele}}(l-k) \exp\left[it(\omega_l - \omega_k)\right] \\ &\quad + \sum_{k,l=-N/2}^{N/2-1} h^*_{\mathrm{opt}}(k) \left[s_y(k) + n_y(k)\right]^* h_{\mathrm{opt}}(l) \cdot \\ &\quad \left[s_y(l) + n_y(l)\right] h_{\mathrm{ele}}(l-k) \exp\left[it(\omega_l - \omega_k)\right] \}, \end{aligned} \quad (1)$$

where κ is receiver's conversion factor and "*" denotes complex conjugation. By defining $w_{kl}(t) \equiv \kappa h^*_{\mathrm{opt}}(k) h_{\mathrm{opt}}(l) h_{\mathrm{ele}}(l-k) \exp\left[it(\omega_l - \omega_k)\right]$ and substituting into Eqn. (1), we obtain

$$\begin{aligned} y(t) &= \sum_{k,l=-N/2}^{N/2-1} \left[s_x(k) + n_x(k)\right]^* w_{kl}(t) \left[s_x(l) + n_x(l)\right] \\ &\quad + \sum_{k,l=-N/2}^{N/2-1} \left[s_y(k) + n_y(k)\right]^* w_{kl}(t) \left[s_y(l) + n_y(l)\right]. \end{aligned}$$

We introduce a partitioned vector by concatenating the real and imaginary parts of Fourier coefficients:

$$\begin{aligned} \mathbf{s}_x &= [s_{x,R}(-N/2), \ldots, s_{x,R}(N/2-1), \\ &\quad s_{x,I}(-N/2), \ldots, s_{x,I}(N/2-1)]^T, \end{aligned} \quad (2)$$

and defining vectors $\mathbf{s}_y$, $\mathbf{n}_x$, and $\mathbf{n}_y$ similarly, we can write

$$y(t) = (\mathbf{s}_x + \mathbf{n}_x)^T \mathbf{W}(t)(\mathbf{s}_x + \mathbf{n}_x) + (\mathbf{s}_y + \mathbf{n}_y)^T \mathbf{W}(t)(\mathbf{s}_y + \mathbf{n}_y),$$

where

$$\mathbf{W} = \begin{bmatrix} \mathbf{F}_R & -\mathbf{F}_I \\ \mathbf{F}_I & \mathbf{F}_R \end{bmatrix} = \mathbf{W}^T,$$

with submatrix $\mathbf{F}$ defined as

$$\begin{bmatrix} w_{-N/2,-N/2} & w_{-N/2,-N/2+1} & \cdots & w_{-N/2,N/2-1} \\ w_{-N/2+1,-N/2} & w_{-N/2+1,-N/2+1} & \cdots & w_{-N/2+1,N/2-1} \\ \vdots & \vdots & \vdots & \vdots \\ w_{N/2-1,-N/2} & w_{N/2-1,-N/2+1} & \cdots & w_{N/2-1,N/2-1} \end{bmatrix}.$$

Let $\mathbf{W} = \mathbf{C}^T \mathbf{\Lambda} \mathbf{C}$ with $\mathbf{\Lambda} = \mathrm{diag}(\lambda_1, \lambda_2, \ldots, \lambda_{2N})$. The $2N \times 2N$ covariance matrices of the input optical noise in the two polarization states are defined as $\mathbf{K}_x = E\{\mathbf{n}_x \mathbf{n}_x^T\}$ and $\mathbf{K}_y = E\{\mathbf{n}_y \mathbf{n}_y^T\}$. Assuming that the optical noise is unpolarized and has variance σ^2, we write $\mathbf{K}_x = \mathbf{K}_y = \mathrm{diag}(\sigma^2, \ldots, \sigma^2)$. Using the linear transformations $\mathbf{u}_x = \mathbf{C}\mathbf{s}_x$, $\mathbf{u}_y = \mathbf{C}\mathbf{s}_y$, $\mathbf{v}_x = \mathbf{C}\mathbf{n}_x$, and $\mathbf{v}_y = \mathbf{C}\mathbf{n}_y$, we can write

$$\begin{aligned} y(t) &= (\mathbf{u}_x + \mathbf{v}_x)^T \mathbf{\Lambda} (\mathbf{u}_x + \mathbf{v}_x) + (\mathbf{u}_y + \mathbf{v}_y)^T \mathbf{\Lambda} (\mathbf{u}_y + \mathbf{v}_y) \\ &= \sum_{k=1}^{2N} q_x(k) + \sum_{k=1}^{2N} q_y(k), \end{aligned}$$

where $q_x(k) = \sum_{k=1}^{2N} \lambda_k \left[u_x^2(k) + 2u_x(k)v_x(k) + v_x^2(k)\right]$, and $q_y(k) = \sum_{k=1}^{2N} \lambda_k [u_y^2(k) + 2u_y(k)v_y(k) + v_y^2(k)]$ where $u_x(k)$, $v_x(k)$, $u_y(k)$, and $v_y(k)$ denote the elements of $\mathbf{u}_x$, $\mathbf{v}_x$, $\mathbf{u}_y$ and $\mathbf{v}_y$, respectively. Since the variables $v_x(k)$ and $v_y(k)$ are Gaussian-distributed with zero mean and unit variance, can be evaluated as

$$\begin{aligned} \Phi_{q_x(k)}(\xi) &= \int_{-\infty}^{+\infty} \exp[i\xi q_x(k)] f_{v_x}(v_x(k)) dv_x(k) \\ &= \frac{1}{\sqrt{1 - 2i\lambda_k \xi}} \exp\left[-\frac{i\lambda_k u_x^2(k)\xi}{1 - 2i\lambda_k \xi}\right], \end{aligned}$$

and similarly for $\Phi_{q_y(k)}(\xi)$.

Since $v_x(k)$ and $v_y(k)$ are independent random variables, so are $q_x(k)$ and $q_y(k)$. Hence, the characteristic function of the output electrical current at the filter output can be written as

$$\begin{aligned}\Phi_y(\xi) &= \prod_{k=1}^{2N} \Phi_{q_x(k)}(\xi) \prod_{k=1}^{2N} \Phi_{q_y(k)}(\xi) \\ &= \prod_{k=1}^{2N} \frac{1}{1-2i\lambda_k\xi} \exp\left[i\xi \sum_{k=1}^{2N} \frac{\lambda_k(u_x^2(k)+u_y^2(k))}{1-2i\lambda_k\xi} \right].\end{aligned}$$

Inversion of the characteristic function $\Phi_y(\xi)$ yields the pdf

$$f_y(y(t)) = \frac{1}{2\pi} \int_{-\infty}^{+\infty} \Phi_y(\xi) \exp\left[-iy(t)\xi\right] d\xi. \quad (3)$$

To obtain the pdf of the electrical current $f_y(y(t))$ in our simulations, we proceed as follows: Calculate (1) the Fourier coefficients of the two polarization states for $S(t)$ and $N(t)$, (2) the optical noise covariance matrices $\mathbf{K}_x$ and $\mathbf{K}_y$, (3) the pdfs for each polarization state by inverting the characteristic functions $\prod_{k=1}^{2N} \Phi_{q_x(k)}(\xi)$ and $\prod_{k=1}^{2N} \Phi_{q_y(k)}(\xi)$, and (4) the pdf of the electrical current $f_y(y(t))$ by convolving the pdfs obtained in step 3.

4. MAP EQUALIZER

We use y_n to denote the sampled electrical current $y(t)$ in the n-th bit after clock recovery, and x_n the corresponding transmitted information bit. We assume that the PMD-induced pulse spreading does not extend beyond the immediate neighboring bit slots, *i.e.*, the pulse spreading of x_n due to PMD is well contained inside the received three-bit sequence (y_{n-1}, y_n, y_{n+1}). In most optical communications systems, the probability that this assumption will be violated is a very small, because the DGD is Maxwellian distributed. For practicality, here we test the performance of a 3-bit MAP equalizer. Extension to longer sequence MAP equalizers using the general form of pdf given in Eqn. (3) is straightforward.

To derive the 3-bit MAP equalizer, write the probability $P(x_n = A_m |\, y_n, y_{n+1}) = P(y_n, y_{n+1}|x_n = A_m)P(x_n = A_m)/P(y_n, y_{n+1})$ where A_m is either "1" or "0". Since the denominator of the equation is common to all probabilities, the MAP criterion is equivalent to choosing the value of x_n to maximize the numerator. Using iterative summations, the criterion for decision for the current sample can be written as

$$\hat{x}_n = \arg\{\max_{x_n} P(y_n, y_{n+1}|x_n = A_m)\, P(x_n = A_m)\}. \quad (4)$$

Assuming that the symbols are equally probable, the expression to be evaluated can be rewritten as

$$\begin{aligned}\hat{x}_n &= \arg\{\max_{x_n} \sum_{x_{n+1}} (P(y_n|x_{n-1}, x_n, x_{n+1}) \\ &\quad \sum_{x_{n+2}} P(y_{n+1}|x_n, x_{n+1}, x_{n+2})\ )\ \}.\end{aligned}$$

In implementation, the conditional pdf $f_y(y_n|x_{n-1}, x_n, x_{n+1})$ can be obtained by transmitting a known training sequence. Using the method described in Section 3, the conditional pdfs of all eight bit patterns of interest can be computed from measurements of the noise-free optical signal and the optical signal-to-noise ratio. The conditional probabilities $P(y_n|\, x_{n-1}, x_n, x_{n+1})$ can then be calculated to be used in the MAP equalizer. In Fig. 1, we show a comparison between the conditional pdfs calculated using Eqn. (3) and the pdfs obtained using Monte Carlo simulations with a total of 8 million bits using the configuration described in Section 5 with a mean DGD value of 57 ps. The calculated conditional pdfs agree very well with the actual pdfs generated by Monte Carlo simulations. In particular, the calculated conditional pdfs can be used to accurately compute the probability of the rare events in the tails of the distribution, which in practice, is not feasible using Monte Carlo simulations. The conditional pdf that is used by the MAP equalizer for PMD compensation needs to be updated on the slow time scale on which the random realization of the fiber PMD changes. As we demonstrate in the next section, the MAP equalizer is very effective in mitigating PMD.

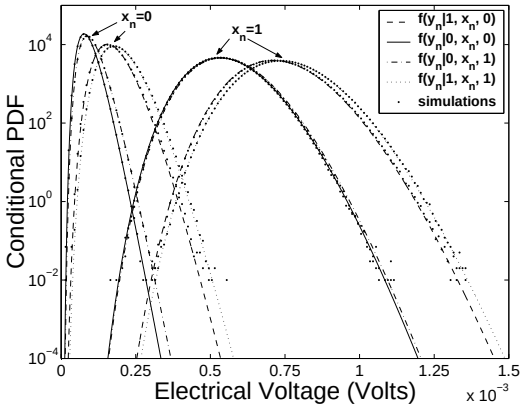

Fig. 1. Comparison between the conditional pdfs calculated using Eqn. (3) and the pdfs from Monte Carlo simulations (denoted by solid dots).

5. SIMULATION RESULTS

Our numerical simulation results are for a 10 Gbits/s return-to-zero (RZ) transmission system using Gaussian pulses with a full width at half maximum of 50 ps. To include the effects of ISI due to all-order PMD, a 1000 km fiber is used, which is modeled by 800 sections of polarization maintaining fiber with a random polarization transformation between each section [6]. ASE noise is added in the optical domain. Fiber nonlinearity and chromatic dispersion are considered small so that they can be neglected. After the fiber propagation and optical amplification, the distorted optical signal – in two polarization states – is filtered by a Gaussian optical filter with a bandwidth of 80 GHz. The signal is then detected by a photodetector and is passed through an

8 GHz 5th order electrical Bessel filter. The electrical current is sampled after clock recovery and the conditional pdfs shown in Fig. 1 are used to generate the conditional cdfs which are stored in a look-up table to be used in the MAP-equalizer.

To evaluate the degree to which the three-bit MAP equalizer compensates for the all-order PMD distortion in the optical fiber, in Fig. 2 we compare the bit-error-rate (BER) obtained using an adaptive threshold with that obtained using the MAP equalizer for a fixed fiber realization as the optical signal-to-noise ratio (OSNR) varies from 0 to 14 dB. We show the bit-error-rate (BER) obtained using the adaptive threshold computed both from Monte Carlo simulations and from the analytical pdfs. We set the PMD parameter of the fiber to be 1.8 $\mathrm{ps}/\sqrt{\mathrm{km}}$, and selected a fixed fiber realization with a DGD of 57 ps, which, in this case, is approximately the mean of the Maxwellian distribution of the DGD. We performed a Monte Carlo simulation using an 8 bit pseudo-random sequence with 10^7 different noise realizations. Given a fiber realization and an OSNR, we used the averages of the analytical conditional pdfs of the ONEs and ZEROs to adaptively select the threshold current so as to minimize the BER. When the OSNR is around 12 dB, the BER with the MAP equalizer is more than two orders of magnitude smaller than with the adaptive threshold. The slopes of the two BER curves suggest that the improvement in the BER will be even greater for larger values of the OSNR.

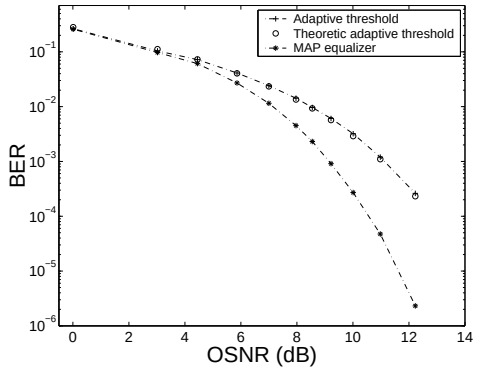

Fig. 2. BER as a function of OSNR with the MAP equalizer and adaptive thresholding.

To study the performance of the MAP equalizer for fibers with different DGD values, we selected six fiber realizations from distributions with mean DGD values of 0 ps (no PMD), 19 ps, 42 ps, 57 ps, 84 ps, and 102 ps. In each case, we chose the fiber realization so that the DGD at the center frequency of the optical channel was approximately equal to the mean DGD. For the simulation results shown in Fig. 3, we used an OSNR of 10 dB. When the DGD is small, the BER with the MAP equalizer is only slightly smaller than with adaptive thresholding, which is to be expected since the MAP equalizer is designed for PMD mitigation. With a small DGD, the conditional pdfs of the ONEs are all similar, as are those of all the ZEROs, and the MAP equalizer

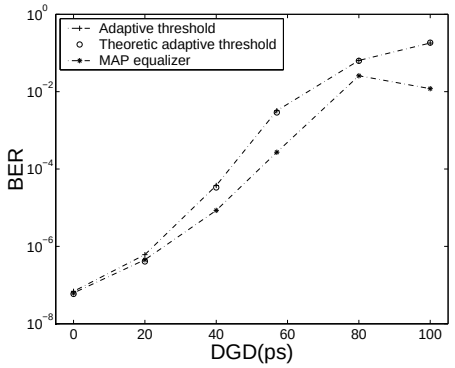

Fig. 3. BER for six different fiber realizations plotted as a function of DGD with the MAP equalizer and adaptive thresholding.

has almost the same function as a normal threshold detector. However, as the DGD increases, the PMD-induced ISI results in different conditional pdfs for the different bits, as we see in Fig. 1. Consequently, the MAP equalizer tends to become more effective as the DGD increases, as we see, for example, when the DGD increases from 19 to 40 to 57 ps. When the DGD is extremely large, for example 100 ps, the PMD-induced ISI may leak beyond the immediate neighboring bits hence breaking our assumption that the ISI is well contained in a three bit pattern. To compensate for very large DGD, the memory length of MAP equalizer may need to be expanded.

Since different fibers selected from a distribution with a fixed mean DGD can result in very different amounts of PMD-induced distortion, to more fully assess the degree to which the MAP equalizer reduces the BER compared to adaptive thresholding, we will need to gather performance statistics from Monte Carlo simulations with a large number of different fiber realizations.

6. REFERENCES

[1] T. Adali, W. Wang, A. Lima, "Electronic equalization in optical fiber communications," in *Proc ICASSP2003*, HongKong, IV497.

[2] H. Bülow, "Electronic equalization of transmission impairments," in *Proc. OFC 2002*, Anaheim, CA, TuF.

[3] H. Bülow and G. Thielecke, "Electronic PMD mitigation - from linear equalization to maximum-likelihood detection," in *Proc. OFC 2001*, Anaheim, CA, WAA3.

[4] H. F. Haunstein, K. Sticht, A. Dittrich, W. Sauer-Greff, and R. Urbansky, "Design of near optimum electrical equalizers for optical transmission in the presence of PMD," in *Proc. OFC 2001*, Anaheim, CA, WAA4.

[5] R. Holzlhner,V. S. Grigoryan, C. R. Menyuk, and W. L. Kath, "Accurate calculation of eye diagrams and bit error rates in optical transmission systems using linearization" *J. Lightwave Tech.*, vol. 20, pp. 389-400, March. 2002.

[6] D. Marcuse, C. R. Menyuk, and P. K. A. Wai, "Application of the Manakov-PMD equation to studies of signal propagation in optical fibers with randomly varying birefringence," *J. Lightwave Tech.*, vol. 15, pp. 1735-1746, Sep. 1997.

[7] C. D. Poole and J. Nagel, *Optical Fiber Telecommunication*, Academic Press, III-A; San Diego, CA, 1997.